Paulo Alexander Jacobsen Jardim
Mechanical and Marine Engineering,
Western Norway University of Applied Sciences (HVL),
Buheilia 3,
Søgne 4640, Norway
e-mail: alexander_jardim@hotmail.com

Jan Tore Rein
Mechanical and Marine Engineering,
Western Norway University of Applied Sciences (HVL),
Sandviksveien 23,
Bergen 5036, Norway
e-mail: jantore@reins.no

Øystein Haveland
Mechanical and Marine Engineering,
Western Norway University of Applied Sciences (HVL),
Gulafjordvegen 1163,
Dalsøyra 5960, Norway
e-mail: oyshav@gmail.com

Thorstein R. Rykkje
Mechanical and Marine Engineering,
Western Norway University of Applied Sciences (HVL),
Kristofer Jansons vei 71B,
Bergen 5089, Norway
e-mail: try@hvl.no

Thomas J. Impelluso
Mechanical and Marine Engineering,
Western Norway University of Applied Sciences (HVL),
Inndalsveien 28,
Bergen 5063, Norway
e-mail: tjm@hvl.no

Modeling Crane-Induced Ship Motion Using the Moving Frame Method

A decline in oil-related revenues challenges Norway to focus on new types of offshore installations. Often, ship-mounted crane systems transfer cargo or crew onto offshore installations such as floating windmills. This project analyzes the motion of a ship induced by an onboard crane in operation using a new theoretical approach to dynamics: the moving frame method (MFM). The MFM draws upon Lie group theory and Cartan's moving frames. This, together with a compact notation from geometrical physics, makes it possible to extract the equations of motion, expeditiously. While others have applied aspects of these mathematical tools, the notation presented here brings these methods together; it is accessible, programmable, and simple. In the MFM, the notation for multi-body dynamics and single body dynamics is the same; for two-dimensional (2D) and three-dimensional (3D), the same. Most importantly, this paper presents a restricted variation of the angular velocity to use in Hamilton's principle. This work accounts for the masses and geometry of all components, interactive motor couples and prepares for buoyancy forces and added mass. This research solves the equations numerically using a relatively simple numerical integration scheme. Then, the Cayley–Hamilton theorem and Rodriguez's formula reconstruct the rotation matrix for the ship. Furthermore, this work displays the rotating ship in 3D, viewable on mobile devices. This paper presents the results qualitatively as a 3D simulation. This research demonstrates that the MFM is suitable for the analysis of "smart ships," as the next step in this work.
[DOI: 10.1115/1.4042536]

Introduction

Norway faces a decrease in revenues from the petroleum industry. Therefore, it is important to look for other means of developing and exploiting renewable energy sources, such as wind and wave energy. To harness wind energy, windmill farms are placed offshore. To service these installations, a ship-mounted crane is used to transfer cargo and engineers. In this kind of operation, precise and accurate crane maneuvering is critical. The crane-induced ship movements, influenced by various weather conditions and waves, lead to difficulties in positioning the load. Many companies solve these problems by using pilots with the skills to compensate for the yaw, pitch, roll, and heave of the ship. Newer cranes are equipped with advanced sensors and inertial devices to analyze and compensate for the movements of the ship. These "smart cranes" can be controlled through software, such as MacGregors three-dimensional (3D)-compensated cranes [1]. Another company, Rolls Royce Marine, designs and manufactures cranes with active heave compensation [2], illustrations are given in Figs. 1 and 2.

The previous research on this topic have been conducted by Maczyński and Wojciech [3] and Xu et al. [4]. The work demonstrates two methods for stabilizing the load of an offshore crane, by determining the drive functions of the cranes boom and winch. Although the paper does prove quantitative results through numeric simulation, it does not present any qualitative visualization and it does not validate them through numerical simulation. Furthermore, their approach relies on commercial/legacy software that is not amenable to infusion with artificial intelligence modules. A method is needed that can be easily coded.

In addition, there is the advent of automated ships. For example, the electrical containership YARA Birkeland will sail fully autonomous between three ports in southern Norway by 2020 [5]. The authors present a dynamic simulation scheme to analyze an active roll reduction system consisting of free-flooding tanks and vacuum pumps. However, while this paper only accounts for the roll of the ship, our paper additionally accounts for the pitch and yaw.

Autonomous ships have several advantages compared to traditional ships. They will be able to sail without any crew onboard. This will increase the safety when sailing under demanding conditions. Such efficiency can also reduce emissions. Some autonomous ships will even be fully electric, supplied with power from onboard battery packages. A fully automated crane needs a

Contributed by the Ocean, Offshore, and Arctic Engineering Division of ASME for publication in the Journal of Offshore Mechanics and Arctic Engineering. Manuscript received July 21, 2018; final manuscript received January 6, 2019; published online February 18, 2019. Assoc. Editor: Zhen Gao.

comprehensive suite of software to be able to analyze and process the information from all the sensors. It needs to conduct motion analysis of the ship movements in real time to be able to operate as efficiently as possible.

The research reports on the current work to analyze crane-induced ship motion. The work in this paper expands upon the previous work by Nordvik et al. [6] by including motor torques, full 3D analysis, numerical integration, and masses of all elements.

As pedagogy, this paper continues its introduction of the moving frame method (MFM). The MFM obviates complexities introduced by an injudicious use of vector algebra in 3D dynamics. Three undergraduate students conducted this work and this demonstrates the power of the MFM.

However, the MFM is not merely pedagogical, for it also investigates the power of Lie Group Theory, Cartan's moving frames, and a new mathematical approach. By itself, this is research.

Finally, this work demonstrates how the 3D web can supplement engineering analyses with visualization on mobile devices.

The one caveat we extend is that the mathematics, while fundamentally simple is extensive heavy with notation. Thus, we will summarize salient mathematical aspects to encourage readers, programmers, and analysts to see the power of this method.

While this paper also presents a software tool, we do not desire that analysts use this tool. Rather, this paper demonstrates how the MFM can enable analysts and designers to rapidly construct their own software tools and avoid expensive simulation software.

Finally, this work demonstrates how the 3D web can supplement engineering analyses.

Should the reader desire, he or she may find a detailed introduction to the MFM in Refs. [7] and [8], along with pedagogical assessment of student learning. Allow us to bullet point the fundamental points of the MFM:

- We exploit the algebra and group theory of Sophus Lie. However, we reduce it to simple matrix methods to enable a rapid transition to programming.
- We exploit the notion of Elie Cartan, that each object has its own moving frame; we use this to formulate the principles of dynamics from the viewpoint of a moving observer—the crane and ship at sea.
- We exploit a new notation developed in Geometrical Physics. This notation enables us to view rotation matrices as operators on columns of vector components.
- We exploit a restriction of the variation of the angular velocity. This enables us to formulate the proper form of the Principle of Virtual Work so as to extract the differential equations of motion using analytical mechanics.
- We apply all of this to the study of crane induced ship motion.
- We visualize the results on the 3D web using WebGL. The reader can move the crane on the ship to study its effect on pitch, roll and yaw in order to design a ship/crane system more efficiently.

The Moving Frame Method

The Norwegian mathematician Marius Sophus Lie (1842–1899) developed Lie Group theory to study the symmetric properties of differential equations. However, the smoothness and continuous nature of such groups make them ideal to model continuous rotations. The MFM exploits Lie Group theory and the Special Orthogonal Group to model rotations. The MFM also makes use of the Special Euclidean group that is a group of mathematical structures that include the position and orientation of bundled into one structure.

The MFM also makes use of the work of Elie Joseph Cartan (1869–1951). Cartan [9] suggested modeling the change of a frame in terms of the frame itself. In this project, we place a moving frame on the ship, the crane tower and the distal crane arm.

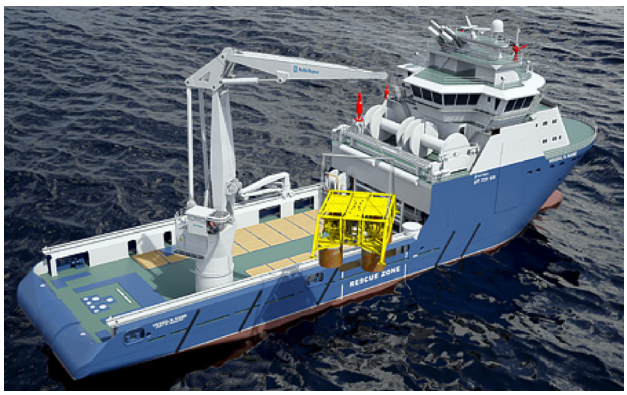

Fig. 1 Dual Drag Link crane, Rolls Royce Marine

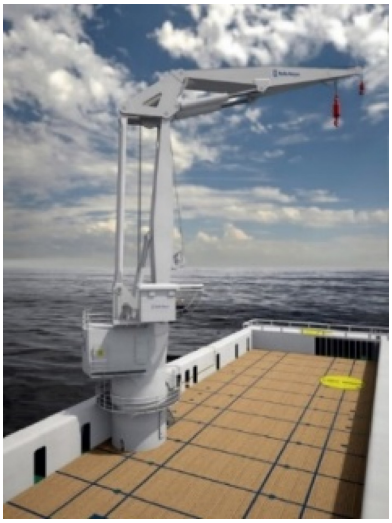

Fig. 2 Close-up of Dual Drag Link crane, Rolls Royce Marine

Finally, the MFM uses a new compact notation from the Geometry of Physics, espoused by the American mathematician Theodore Frankel (1929–2017) [10]. This notation enables us to view rotation matrices as operators on components of vectors.

Murray et al. [11] suggested this use aspects of Lie Algebra and Group Theory. However, while their approach is sometimes difficult for graduate students, the MFM is readily comprehensible to undergraduates [7,8]. Thus, this current work extends their efforts by also proposing a restriction on the variation of the angular velocity. By exploiting the algebra of se(3) and ensuring the

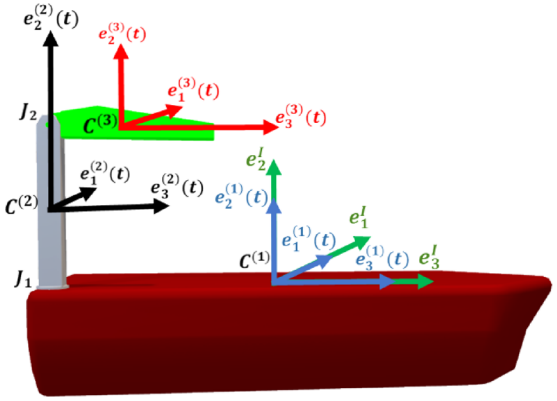

Fig. 3 Model and frames

commutativity of mixed partials in the variational process, this work delivers a natural restriction on the variation of the angular velocity to be used in Hamilton's principle and its associated principle of virtual work [12].

Absolute Ship Rotation. The analysis commences with the first body, the ship itself, presented in Fig. 3. From the ship, there is a systematic progression to the column of the crane (colored gray) and then the remote arm (colored green). We supply each body with a Cartesian frame (four frames when also including the inertial frame). We number the frames in ascending order, starting with the ship and up to the second, distal, arm as the third frame.

The multibody system consists of three linked bodies. The ship is body 1, the tower of the crane is body 2, and the distal manipulator arm is body 3. Each individual body is endowed with its own moving Cartesian coordinate system: $s_C^{(\alpha)}(t) = \left\{ s_1^{(\alpha)} \;\; s_2^{(\alpha)} \;\; s_3^{(\alpha)} \right\}^T$, where the superscript $\alpha = 1$, 2, or 3.

Next, we define a body frame by partial derivatives of the coordinate functions, wherein each basis vector is tangent to the coordinate function

$$\left(\mathbf{e}_1^{(\alpha)}(t) \quad \mathbf{e}_2^{(\alpha)}(t) \quad \mathbf{e}_3^{(\alpha)}(t) \right)^{\mathrm{T}} \equiv \left(\partial/\partial s_1^{(\alpha)} \quad \partial/\partial s_2^{(\alpha)} \quad \partial/\partial s_3^{(\alpha)} \right)^{\mathrm{T}} \tag{1}$$

Here, $\mathbf{e}^{(\alpha)}(t) = \left(\mathbf{e}_1^{(\alpha)}(t)\, \mathbf{e}_2^{(\alpha)}(t)\, \mathbf{e}_3^{(\alpha)}(t) \right)$ is a time-dependent moving frame, associated with the moving body.

We deposit an inertial frame from the first body, at the start of the analysis $(t = 0)$

$$\left(\mathbf{e}_1^I \quad \mathbf{e}_2^I \quad \mathbf{e}_3^I \right)^{\mathrm{T}} = \left(\mathbf{e}_1^{(\alpha)}(0) \quad \mathbf{e}_2^{(\alpha)}(0) \quad \mathbf{e}_3^{(\alpha)}(0) \right)^{\mathrm{T}} \tag{2}$$

The inertial frame does not rotate or accelerate. This frame is fixed. Using a superposed dot to indicate time differentiation, this implies $\dot{\mathbf{e}}^I = 0$.

The ship will rotate (pitch, yaw, and roll). The moving ship frame rotates from the inertial frame as

$$\mathbf{e}^{(1)}(t) = \mathbf{e}^{\mathrm{I}} R^{(1)}(t) \tag{3}$$

In full matrix from, Eq. (3) represents

$$\left(\mathbf{e}_1^{(1)}(t) \quad \mathbf{e}_2^{(1)}(t) \quad \mathbf{e}_3^{(1)}(t) \right) = \left(\mathbf{e}_1^I \quad \mathbf{e}_2^I \quad \mathbf{e}_3^I \right) \begin{bmatrix} R_{11}(t) & R_{12}(t) & R_{13}(t) \\ R_{21}(t) & R_{22}(t) & R_{23}(t) \\ R_{31}(t) & R_{32}(t) & R_{33}(t) \end{bmatrix} \tag{4}$$

The rotation matrix for the ship is a full matrix and we will find its components during the numerical integration process. The time rate of the ship frame rotation is

$$\dot{\mathbf{e}}^{(1)}(t) = \mathbf{e}^{\mathrm{I}} \dot{R}^{(1)}(t) \tag{5}$$

Rotation matrices are members of the special orthogonal group, SO(3). As such, their inverse is their transpose. Thus, we assert the inverse of Eq. (3)

$$\mathbf{e}^{\mathrm{I}} = \mathbf{e}^{(1)}(t) \left(R^{(1)}(t) \right)^{\mathrm{T}} \tag{6}$$

We insert Eq. (5) into Eq. (6) to obtain

$$\dot{\mathbf{e}}^{(1)}(t) = \mathbf{e}^{(1)}(t) \left(R^{(1)}(t) \right)^{\mathrm{T}} \dot{R}^{(1)}(t) \tag{7}$$

The algebra of so(3) is such that $\left(R^{(1)}(t) \right)^{\mathrm{T}} \dot{R}^{(1)}(t)$ is a skew symmetric matrix. We define this product as the angular velocity *matrix* and it is of the following form:

$$\tilde{\omega}^{(1)}(t) = \left(R^{(1)}(t) \right)^{\mathrm{T}} \dot{R}^{(1)}(t) = \begin{bmatrix} 0 & -\omega_3^{(1)} & \omega_2^{(1)} \\ \omega_3^{(1)} & 0 & -\omega_1^{(1)} \\ -\omega_2^{(1)} & \omega_1^{(1)} & 0 \end{bmatrix} \tag{8}$$

Thus, the time rate of change of the first frame becomes

$$\dot{\mathbf{e}}^{(1)}(t) = \mathbf{e}^{(1)}(t) \tilde{\omega}^{(1)}(t) \tag{9}$$

We define the expression in Eq. (9) as the *angular velocity matrix*. By formulating these terms as a skew symmetric matrix, the direct results of the algebra of se(3), we can apply all operations as matrices without resorting to the cross product. However, if desired, we may take the elements of the skew symmetric matric, construct a column of coordinates ("*unskewing*" the components), and associate it with the same moving frame

$$\boldsymbol{\omega}^{(1)}(t) = \mathbf{e}^{(1)}(t) \begin{pmatrix} \omega_1^{(1)}(t) \\ \omega_2^{(1)}(t) \\ \omega_3^{(1)}(t) \end{pmatrix} \tag{10}$$

Dynamics was constructed and deployed vectors to model rotations. However, vectors cannot model rotations out of the plane without severe notational interventions that confound students and complicate coding. Furthermore, we see that the frame for the angular velocity vector is time dependent. It relates to other frames through rotation matrices.

Relative Rotation. Orthogonal rotation matrices also relate the orientation of two moving frames. In the following, for relative motion of one frame from another moving frame, we will adopt a superscript notation: $(\alpha + 1/\alpha)$. While this may appear ambiguous, it is less disconcerting that the more burdensome notation: $\left((\alpha + 1)/\alpha\right)$. We ask the reader's indulgence to use this shortened form and its inverse

$$\mathbf{e}^{(\alpha+1)}(t) = \mathbf{e}^{(\alpha)}(t) R^{(\alpha+1/\alpha)}(t) \tag{11}$$

$$\mathbf{e}^{(\alpha)}(t) = \mathbf{e}^{(\alpha+1)}(t) \left(R^{(\alpha+1/\alpha)}(t) \right)^{\mathrm{T}} \tag{12}$$

By utilizing the closure property of the SO(3) group (the product of two rotation matrices is a rotation matrix), this can also be expressed in the inertial frame

$$\mathbf{e}^{(\alpha+1)}(\mathrm{t}) = \mathbf{e}^I R^{(\alpha)}(\mathrm{t}) R^{(\alpha+1/\alpha)}(\mathrm{t}) = \mathbf{e}^I R^{(\alpha+1)}(\mathrm{t}) \tag{13}$$

Ship Translation. We represent *absolute* position coordinates from an *inertial* frame with "*x*." The subscript "c" designates that we are locating the center of mass of the boat

$$\mathbf{r}_C^{(1)}(t) = \left(\mathbf{e}_1^I \quad \mathbf{e}_2^I \quad \mathbf{e}_3^I \right) \begin{pmatrix} x_{1C}^{(1)}(\mathrm{t}) \\ x_{2C}^{(1)}(\mathrm{t}) \\ x_{3C}^{(1)}(\mathrm{t}) \end{pmatrix} = \mathbf{e}^I x_C^{(1)}(\mathrm{t}) \tag{14}$$

Translational velocity coordinates from an inertial frame are

$$\boldsymbol{v}_C{}^{(1)}(t) = \dot{\boldsymbol{r}}_C{}^{(1)}(t) = \boldsymbol{e}^I \dot{x}_C{}^{(1)}(t) \tag{15}$$

We continue to place the frame as a row vector before the components. With this notation, we view the rotation matrices as matrix operators on columns of components.

Crane Translation. We represent *relative* translational position coordinates from a *moving* frame with "*s*" and an appropriate superscript.

The vector $s_C{}^{(2/1)}$ represents the distance between the center of mass of the crane tower and the center of mass of the ship (hence the subscript "c"); it is formulated in the moving body-1 frame. We express this vector in the moving boat frame. Furthermore, the coordinates to locate the crane, from the body-1 frame, are not time-dependent

$$s_C{}^{(2/1)}(t) = \begin{pmatrix} \mathbf{e}_1^{(1)}(\mathrm{t}) & \mathbf{e}_2^{(1)}(\mathrm{t}) & \mathbf{e}_3^{(1)}(\mathrm{t}) \end{pmatrix} \begin{pmatrix} s_{1C}^{(2/1)} \\ s_{2C}^{(2/1)} \\ s_{3C}^{(2/1)} \end{pmatrix} = \mathbf{e}^{(1)}(t) s_c{}^{(2/1)} \tag{16}$$

Finally, to locate the absolute location of a center of mass on a child body, we first proceed to the parent in the inertial frame and then accumulate the distance to the child, in the parent frame

$$\mathbf{r}_C^{(2)}(t) = \mathbf{r}_C^{(1)}(t) + \mathbf{e}^{(1)}(t) s_C^{(2/1)} \tag{17}$$

Absolute Frame Connections Matrices and SE(3). This section presents the structuring of both the rotation and displacement in one expression. By structuring rotation and translations together, one obtains a homogeneous transformation matrix. Denavit and Hartenberg [13] were the first to use homogeneous transformation matrices, but they did not recognize at the time that such transformations were members of the special Euclidean group, denoted as SE(3). The reader may find a more thorough development of the following theory in Ref. [14].

We define a frame connection as a bundle of a frame and the frame's position. Below, we present two frame connections. The first one defines the inertial origin

$$(\mathbf{e}^I \; \mathbf{0}) = \begin{pmatrix} \mathbf{e}_1^I & \mathbf{e}_2^I & \mathbf{e}_3^I & \mathbf{0} \end{pmatrix} \tag{18}$$

The second one represents a frame connection for a moving frame: the frame and its position from the inertial origin

$$\left(\mathbf{e}^{(\alpha)}(t) \; \mathbf{r}_C^{(\alpha)}(t)\right) = \begin{pmatrix} \mathbf{e}_1^{(\alpha)}(t) & \mathbf{e}_2^{(\alpha)}(t) & \mathbf{e}_3^{(\alpha)}(t) & \mathbf{r}_C^{(\alpha)}(t) \end{pmatrix} \tag{19}$$

We define a frame connection matrix $E^{(\alpha)}(t)$ to relate these two expressions in one structure. This matrix accounts for rotation and translation. Let 0_3 represent a 3×1 column zero vector. Let $x_C^{(\alpha)}(\mathrm{t})$ denote the column coordinates with respect to the inertial frame. Thus

$$E^{(\alpha)}(t) = \begin{bmatrix} R^{(\alpha)}(t) & x_C^{(\alpha)}(t) \\ 0_3^T & 1 \end{bmatrix} \tag{20}$$

With this frame connection matrix, we relate the moving and inertial frame connections

$$\left(\mathbf{e}^{(\alpha)}(t) \; \mathbf{r}_C^{(\alpha)}(t)\right) = (\mathbf{e}^I \; \mathbf{0}) E^{(\alpha)}(t) \tag{21}$$

This expanded matrix exploits the power of the SE(3) group and is what enables the rapid extraction of the equations of motion.

The element in Eq. (20) is a member of the special Euclidean group and its inverse is known

$$E^{(\alpha)}(t)^{-1} = \begin{bmatrix} R^{(\alpha)}(t)^{-1} & -R^{(\alpha)}(t)^{-1} x_C^{(\alpha)}(t) \\ 0_3^T & 1 \end{bmatrix} \tag{22}$$

$$(\mathbf{e}^I \; 0) = \left(\mathbf{e}^{(\alpha)}(t) \; \mathbf{r}_C^{(\alpha)}(t)\right) E^{(\alpha)}(t)^{-1} \tag{23}$$

Relative Frame Connections Matrices and SE(3). We now set aside how SE(3) is used to relate moving and inertial frames and turn to relations between two moving frames, e.g., crane arm and ship.

The relation between the child $(\alpha+1)$-frame and the parent body-α-frame is expressed using the *relative* frame connection matrix $E^{(\alpha+1/\alpha)}$ (where, once again, we resort to "s" for a coordinate that will be expressed in a moving frame)

$$E^{(\alpha+1/\alpha)}(t) = \begin{bmatrix} R^{(\alpha+1/\alpha)}(t) & s_C^{(\alpha+1/\alpha)}(t) \\ 0_3^T & 1 \end{bmatrix} \tag{24}$$

Thus, we can assert

$$\left(\mathbf{e}^{(\alpha+1)}(t) \; \mathbf{r}_C^{(\alpha+1)}(t)\right) = \left(\mathbf{e}^{(\alpha)}(t) \; \mathbf{r}_C^{(\alpha)}(t)\right) E^{(\alpha+1/\alpha)}(t) \tag{25}$$

Again, the closure property of SE(3) informs us that the absolute frame connection matrix of the $(\alpha+1)$-body—the product of the absolute frame connection matrix of body-α and the relative frame connection matrix for the two bodies—is also a member of SE(3)

$$E^{(\alpha+1)}(\mathrm{t}) = E^{(\alpha)}(\mathrm{t}) E^{(\alpha+1/\alpha)}(\mathrm{t}) \tag{26}$$

Rates of Frame Connections Matrices and SE(3).

Continuing, we take the time derivative of Eq. (21)

$$\left(\dot{\mathbf{e}}^{(\alpha)}(t) \; \dot{\mathbf{r}}_C^{(\alpha)}(t)\right) = (\mathbf{e}^I \; 0) \dot{E}^{(\alpha)}(t) \tag{27}$$

We use the orthogonality relationship in Eq. (27)

$$\left(\dot{\mathbf{e}}^{(\alpha)}(t) \; \dot{\mathbf{r}}_C^{(\alpha)}(t)\right) = \left(\mathbf{e}^{(\alpha)}(t) \; \mathbf{r}_C^{(\alpha)}(t)\right) E^{(\alpha)-1}(t) \dot{E}^{(\alpha)}(t) \tag{28}$$

We define

$$\Omega^{(\alpha)}(t) = E^{(\alpha)-1}(t) \dot{E}^{(\alpha)}(t) \tag{29a}$$

When multiplied out, this provides an equation for the angular and translational velocity of each body

$$\Omega^{(\alpha)}(t) = E^{(\alpha)-1}(t) \dot{E}^{(\alpha)}(t) = \begin{bmatrix} \overleftrightarrow{\omega}(\alpha) & v_C^{(\alpha)} \\ 0 & 0 \end{bmatrix} \tag{29b}$$

We will see that when multiplying, these terms provide the angular velocity and translational velocity of each body or link, more efficiently.

Kinematics of Ship/Crane System

Now that we have presented the fundamentals, allow us to revisit them in the context of the ship mechanics in this problem as we setup all the kinematic equations.

Kinematics of Body—1: The Ship. As a result of the power of SE(3) and its associated algebra, we can obtain the angular velocity matrix for the ship by multiplying out the terms in Eq. (29). Admittedly, for this first link of the tree, the terms are obvious, but the power of SE(3) manifests itself with later links in this tree

$$\overleftrightarrow{\omega^{(1)}}(t) = \left(R^{(1)}(t)\right)^{\mathrm{T}} \dot{R}^{(1)}(t) \tag{30}$$

In addition, we obtain the linear velocity for the ship in the inertial frame

$$\dot{\boldsymbol{r}}_C^{(1)}(t) = \mathbf{e}^I \dot{x}_c^{(1)}(t) \tag{31}$$

Kinematics of Body 2—Tower. We attach a coordinate frame $\mathbf{e}^{(2)}(t)$ to the center of mass $C^{(2)}$ of the crane tower

$$\mathbf{e}^{(2)}(t) = \begin{pmatrix} \mathbf{e}_1^{(2)}(t) & \mathbf{e}_2^{(2)}(t) & \mathbf{e}_3^{(2)}(t) \end{pmatrix} \tag{32}$$

We find the relative position from $\mathbf{e}^{(1)}(t)$ to $\mathbf{e}^{(2)}(t)$ by first translating from the center of mass $C^{(1)}$ of the ship, to the joint where the rotation happens, then rotating with the crane tower's operation, to obtain the new orientation, and finally, translating from the joint to the center of mass $C^{(2)}$ of the link.

The first translation from $C^{(1)}$ to the joint J_1 is obtained by moving in the three-direction and the one-direction

$$s_{J_1} = \mathbf{e}^{(1)}(t)s_{J_1} = \mathbf{e}^{(1)}(t)\begin{pmatrix} b^{(1)} \\ 0 \\ d^{(1)} \end{pmatrix} \tag{33}$$

At the first joint, the rotation happens about the second axis, which gives the following frame rotation relation:

$$\mathbf{e}^{(2)}(t) = \mathbf{e}^{(1)}(t)R^{(2/1)}(t) = \mathbf{e}^{(1)}(t)\begin{bmatrix} \cos\phi(t) & 0 & \sin\phi(t) \\ 0 & 1 & 0 \\ -\sin\phi(t) & 0 & \cos\phi(t) \end{bmatrix} \tag{34}$$

Finally, the last translation from the joint J_1 to the center of mass of the second body is obtained by moving in the two-direction, half the total length of the tower. This translation is expressed using the $\boldsymbol{e}^{(2)}$-frame

$$s_{C_2} = \mathbf{e}^{(2)}(t)s_{C_2} = \mathbf{e}^{(2)}(t)\begin{pmatrix} 0 \\ l^{(2)} \\ 0 \end{pmatrix} \tag{35}$$

With this information, we may build the frame connection relationships as "do not rotate, but translate, rotate but do not translate, finally translate, but do not rotate"

$$\begin{aligned}\left(\mathbf{e}^{(2)}(t)\mathbf{r}_C^{(2)}(t)\right) &= \left(\mathbf{e}^{(1)}(t)\mathbf{r}_C^{(1)}(t)\right)E^{(2/1)} \\ &= \left(\mathbf{e}^{(1)}(t)\mathbf{r}_C^{(1)}(t)\right)\begin{bmatrix} I & s_{J_1} \\ 0^T & 1 \end{bmatrix}\begin{bmatrix} R^{(2/1)} & 0 \\ 0 & 1 \end{bmatrix}\begin{bmatrix} I & s_{C_2} \\ 0^{\mathrm{T}} & 1 \end{bmatrix}\end{aligned}$$

This provides $E^{(2/1)}$. This in turn with Eq. (28), the group properties of SE(3), and then Eq. (29*b*) enables us to extract

$$\omega^{(2)}(t) = \left(R^{(2/1)}(t)\right)^{\mathrm{T}}\omega^{(1)}(t) + \dot{\phi}^{(2)}e_2 \tag{36}$$

$$\dot{x}_c^{(2)}(t) = R^{(1)}(t)R^{(2/1)}(t)\left(\overleftrightarrow{s_{C_2}}\right)^{\mathrm{T}}\omega^{(2)}(t) + R^{(1)}(t)\left(\overleftrightarrow{s_{J_1}}\right)^{\mathrm{T}}\omega^{(1)}(t) + \dot{x}_c^{(1)}(t) \tag{37}$$

Reference [11] provides all details.

Kinematics of Body 3—Arm. The second link of the crane is the third body of the system. The frame $\boldsymbol{e}^{(3)}$ is attached to the center of mass $C^{(3)}$

$$\boldsymbol{e}^{(3)}(t) = \begin{pmatrix} \boldsymbol{e}_1^{(3)}(t) & \boldsymbol{e}_2^{(3)}(t) & \boldsymbol{e}_3^{(3)}(t) \end{pmatrix} \tag{38}$$

To reach this frame, from the body-2 (tower) frame, we must first translate up the tower. The translation from the center of mass of the second body to the joint connecting the second and third body is s_{J_2}

$$s_{J_2} = \mathbf{e}^{(2)}(t)s_{J_2} = \mathbf{e}^{(2)}(t)\begin{pmatrix} 0 \\ l^{(2)} \\ 0 \end{pmatrix} \tag{39}$$

Next, we must rotate with the distal arm as it lifts and lowers. Here, $R^{(3/2)}$ is the rotation matrix for the relative rotation of the third frame, from the second frame, which happens about the one-axis only

$$R^{(3/2)}(t) = \begin{bmatrix} 1 & 0 & 0 \\ 0 & \cos\xi(t) & -\sin\xi(t) \\ 0 & \sin\xi(t) & \cos\xi(t) \end{bmatrix} \tag{40}$$

Finally, we must translate from the joint to reach the center of mass of the distal arm

$$s_{C_3} = \mathbf{e}^{(3)}(t)s_{C_3} = \mathbf{e}^{(3)}(t)\begin{pmatrix} 0 \\ 0 \\ l^{(3)} \end{pmatrix} \tag{41a}$$

Again, we combine these as

$$\begin{aligned}\left(\mathbf{e}^{(3)}(t)\mathbf{r}_C^{(3)}(t)\right) &= \left(\mathbf{e}^{(2)}(t)\mathbf{r}_C^{(2)}(t)\right)E^{(3/2)} \\ &= \left(\mathbf{e}^{(2)}(t)\mathbf{r}_C^{(2)}(t)\right)\begin{bmatrix} I & s_{J_2} \\ 0^T & 1 \end{bmatrix}\begin{bmatrix} R^{(3/2)} & 0 \\ 0 & 1 \end{bmatrix}\begin{bmatrix} I & s_{C_3} \\ 0^{\mathrm{T}} & 1 \end{bmatrix}\end{aligned} \tag{41b}$$

As previously, Ref. [14] provides the details, but we would then extract

$$\omega^{(3)}(t) = R^{(3/2)\mathrm{T}}(t)R^{(2/1)\mathrm{T}}(t)\omega^{(1)}(t) + \left(R^{(3/2)}(t)\right)^{\mathrm{T}}\dot{\phi}^{(2)}e_2 + \dot{\xi}^{(3)}e_1 \tag{42}$$

$$\dot{x}_c^{(3)}(t) = R^{(1)}(t)\begin{pmatrix} R^{(2/1)}(t)R^{(3/2)}(t)\left(\overleftrightarrow{s_{C_3}}\right)^{\mathrm{T}}\omega^{(3)} + \\ R^{(2/1)}(t)\left(\overleftrightarrow{s_{J_2}}\right)^{\mathrm{T}}\omega^{(2)} + \left(\overleftrightarrow{s_{C_2}}\right)^{\mathrm{T}}\omega^{(1)} \end{pmatrix} + \dot{x}_c^{(1)}(t) \tag{43}$$

We have now obtained all equations needed for the kinematics analysis: Eqs. (30), (31), (36), (37), (42), and (43).

Generalized Coordinates

The velocities and angular velocities for all three bodies are gathered in an 18×1 matrix $\{\dot{X}(t)\}$. We refer to the terms on left in Eq. (44*a*) as the Cartesian coordinate rates.

$$\{\dot{X}(t)\} \equiv \begin{pmatrix} \dot{x}_C^{(1)}(t) \\ \omega^{(1)}(t) \\ \dot{x}_C^{(2)}(t) \\ \omega^{(2)}(t) \\ \dot{x}_C^{(3)}(t) \\ \omega^{(3)}(t) \end{pmatrix} \tag{44a}$$

$$\{\dot{q}(t)\} \equiv \begin{pmatrix} \dot{x}_C^{(1)}(t) \\ \omega^{(1)}(t) \\ \dot{\phi}^{(2)}(t) \\ \dot{\xi}^{(3)}(t) \end{pmatrix} \tag{44b}$$

We wish to reduce this problem to the minimum number of rates of essential generalized coordinates that describe the configuration. These coordinates will be the possible translational and angular velocities of the boat; they also include the angular rate of

the turning of the tower (body-2) and arm (body-3). The *essential* generalized velocities, on the right in Eq. (44*b*), are contained in the 8×1 matrix $\{\dot{q}(t)\}$. These express the essential velocities—three rates and angular velocities for the ship and the essential angles for the crane.

The Cartesian velocities and essential generalized velocities are related linearly through the 18×8 matrix $[B(t)]$

$$\{\dot{X}(t)\} = [B(t)]\{\dot{q}(t)\} \tag{45}$$

Thus, the cells of matrix $[B(t)]$ are constructed from the velocities and angular velocities from all three elements

$$[B(t)] = \begin{bmatrix} I_3 & 0_{3\times3} & 0_{3\times1} & 0_{3\times1} \\ 0_{3\times3} & I_3 & 0_{3\times1} & 0_{3\times1} \\ I_3 & R^{(1)}(t)\left(\overleftrightarrow{s_C^{(2/1)}}\right)^{\mathrm{T}} & 0_{3\times1} & 0_{3\times1} \\ 0_{3\times3} & \left(R^{(2/1)}(t)\right)^{\mathrm{T}} & e_2 & 0_{3\times1} \\ I_3 & B_{52} & B_{53} & B_{54} \\ 0_{3\times3} & \left(R^{(3/1)}(t)\right)^{\mathrm{T}} & \left(R^{(3/2)}(t)\right)^{\mathrm{T}} e_2 & e_1 \end{bmatrix} \tag{46a}$$

$$\begin{aligned} B_{52} &= R^{(1)}(t)\begin{pmatrix} R^{(2/1)}(t)R^{(3/2)}(t)\left(\overleftrightarrow{s_{C_3}}\right)^{\mathrm{T}}\left(R^{(2/1)}(t)\right)^{\mathrm{T}}\left(R^{(3/2)}(t)\right)^{\mathrm{T}} \\ +R^{(2/1)}(t)\left(\overleftrightarrow{s_{J_2}}\right)^{\mathrm{T}}\left(R^{(2/1)}(t)\right)^{\mathrm{T}} + \left(\overleftrightarrow{s_{C_2}}\right)^{\mathrm{T}} \end{pmatrix} \\ B_{53} &= R^{(1)}(t)\begin{pmatrix} R^{(2/1)}(t)R^{(3/2)}(t)\left(\overleftrightarrow{s_{C_3}}\right)^{\mathrm{T}}\left(R^{(3/2)}(t)\right)^{\mathrm{T}} e_2 \\ +R^{(2/1)}(t)\left(\overleftrightarrow{s_{C_2}}\right)^{\mathrm{T}} e_2 \end{pmatrix} \\ B_{54} &= R^{(1)}(t)R^{(2/1)}(t)R^{(3/2)}(t)\left(\overleftrightarrow{s_{C_3}}\right)^{\mathrm{T}} e_1 \end{aligned} \tag{46b}$$

Kinetics of Ship/Crane System

Kinetic Energy. The kinetic energy of the system consists of expressions for the angular and translational kinetic energy for the ship, tower, and arm (bodies 1–3)

$$K^{(\alpha)} = \frac{1}{2}\left(\dot{x}_C^{(\alpha)} L_C^{(\alpha)} + \omega^{(\alpha)} H_C^{(\alpha)}\right) = \frac{1}{2}\left\{m^{(\alpha)}(\dot{x}_C^{(\alpha)})^2 + J_C^{(\alpha)}(\omega^{(\alpha)})^2\right\} \tag{47}$$

Let us define $[\mathrm{M}]$ as a 18×18 block matrix with mass and moment of inertia of the bodies, diagonally partitioned

$$[M] = \begin{bmatrix} m^{(1)}I_3 & 0_3 & 0_3 & 0_3 & 0_3 & 0_3 \\ 0_3 & J_C^{(1)} & 0_3 & 0_3 & 0_3 & 0_3 \\ 0_3 & 0_3 & m^{(2)}I_3 & 0_3 & 0_3 & 0_3 \\ 0_3 & 0_3 & 0_3 & J_C^{(2)} & 0_3 & 0_3 \\ 0_3 & 0_3 & 0_3 & 0_3 & m^{(3)}I_3 & 0_3 \\ 0_3 & 0_3 & 0_3 & 0_3 & 0_3 & J_C^{(3)} \end{bmatrix} \tag{48}$$

Thus, we may write the total kinetic energy in matrix form

$$K = \frac{1}{2}\{\dot{X}\}^T[M]\{\dot{X}\} \tag{49}$$

Hamilton's Principle. Define a Lagrangian L as the following difference between the kinetic energy K and the potential energy U:

$$L \equiv K - U \tag{50}$$

We must obtain a minimization of the *action* in accordance with Hamilton's Principle. We must express the *variation* of the functional and then set the variation to zero. Let us symbolize the process as

$$\delta \int_{t_0}^{t_1} L(q(t), \dot{q}(t))dt = 0 \tag{51}$$

Finally, we will use the principle of virtual work in terms of the essential generalized variables.

Variations. Before proceeding, we will need to take derivatives in the "direction" of the variation to minimize the action. The directional derivatives with ε are called the Gâteaux-derivatives in the functional space theory.

The commutativity of mixed partials readily holds for translational velocity and one must ensure

$$\delta\dot{x}_C^{(\alpha)}(t) = \left(\frac{d}{dt}\delta x_C^{(\alpha)}(t)\right) \tag{52}$$

However, the variation of the angular velocity is restricted in 3D space. This actually mimics the difficulty of using vectors to model 3D rotations. First, we define the following term:

$$\overleftrightarrow{\delta\pi^{(\alpha)}} = (R^{(\alpha)})^{\mathrm{T}}\delta R^{(\alpha)} \tag{53}$$

Equation (53) term does not exist in its unvaried form. It defines the virtual frame-rotation vector $\delta\boldsymbol{\pi}^{(\alpha)}$, in the same way as the angular velocity matrix defined the angular velocity in Eq. (9)

$$\delta\boldsymbol{\pi}^{(\alpha)} = \mathbf{e}^{(\alpha)}\delta\pi^{(\alpha)} \tag{54}$$

By ensuring the commutativity of mixed partials (time and variation with regard to the directional derivative of the variation parameter), we arrive at a restriction. We find that the variation of the angular velocity depends on the virtual frame rotation, referred to as *restricted variation of virtual angular velocity*

$$\delta\omega^{(\alpha)} = \frac{d}{dt}(R^{(\alpha)\mathrm{T}}\delta R^{(\alpha)}) + \overleftrightarrow{\omega}(\alpha)(R^{(\alpha)\mathrm{T}}\delta R^{(\alpha)})_{\text{unskewed}} \tag{55}$$

These (one for each body) are expressed with the body frame. They are conjugate to the moment M expressed with the body frame. Moment versus virtual rotation is a natural pair in the principle of virtual work and yields Euler's equation. This was the weakest point in the classical multibody dynamics. Wittenburg [15,16] postulated the principle of virtual power to use the weighted form of Euler's equation by the virtual angular velocity.

Moment and Omega Define the Power, Not the Work. These results were found by Murakami [12] and independently by Holm [17]. Before continuing, note the similarity between Eqs. (9) and (54). This was the weakest point in the classical multibody dynamics. To take the variation of the Lagrangian in Eq. (50), we collate the unrestricted *virtual generalized displacements* $\{\delta\tilde{X}\}$

$$\{\delta\tilde{X}\} = \begin{pmatrix} \delta x^{(1)} \\ \delta\pi^{(1)} \\ \delta x^{(2)} \\ \delta\pi^{(2)} \\ \delta x^{(3)} \\ \delta\pi^{(3)} \end{pmatrix} \tag{56}$$

The next step is to simplify the relationships in Eqs. (52) and (55). To accomplish this, we first define a term. This term might appear to be a waste of computational space. However, the form of this term enables one to obtain the equations of motion

Table 1 List of coordinates and their relationships

Variation of generalized velocity	Virtual generalized displacement	Virtual generalized velocity	Essential generalized velocities
$\{\delta\dot{X}\} \equiv \begin{Bmatrix} \delta\dot{x}_C^{(1)} \\ \delta\omega^{(1)} \\ \delta\dot{x}_C^{(2)} \\ \delta\omega^{(2)} \\ \vdots \\ \delta\dot{x}_C^{(n)} \\ \delta\omega^{(n)} \end{Bmatrix}$	$\{\delta\tilde{X}(T)\} \equiv \begin{Bmatrix} \delta x_C^{(1)}(t) \\ \delta\pi^{(1)}(t) \\ \delta\dot{x}_C^{(2)}(t) \\ \delta\pi^{(2)}(t) \\ \vdots \\ \delta\dot{x}_C^{(n)}(t) \\ \delta\pi^{(n)}(t) \end{Bmatrix}$	$\{\dot{X}(t)\} \equiv \begin{Bmatrix} \dot{x}_C^{(1)}(t) \\ \omega^{(1)}(t) \\ \dot{x}_C^{(2)}(t) \\ \omega^{(2)}(t) \\ \vdots \\ \dot{x}_C^{(n)} \\ \omega^{(n)} \end{Bmatrix}$	$\{\dot{q}(t)\} \equiv \begin{pmatrix} \dot{x}_C^{(1)}(t) \\ \omega^{(1)}(t) \\ \dot{\phi}^{(2)}(t) \\ \dot{\xi}^{(3)}(t) \end{pmatrix}$

Relating column 2 and variations of column 4: $\{\delta\tilde{X}(t)\} = [B(t)]\{\delta q(t)\}$

Relating column 3 and rates in column 4: $\{\dot{X}\} = [B(t)]\{\dot{q}(t)\}$

Restriction on column 1: $\{\delta\dot{X}\} = \frac{d}{dt}\{\delta\tilde{X}\} + [D]\{\delta\tilde{X}\}$

$$[D] \equiv \begin{bmatrix} 0_{3\times3} & \overleftrightarrow{\omega^{(1)}(t)}_{3\times3} & 0_{3\times3} & 0_{3\times3} & 0_{3\times3} & 0_{3\times3} \\ 0_{3\times3} & 0_{3\times3} & 0_{3\times3} & 0_{3\times3} & 0_{3\times3} & 0_{3\times3} \\ 0_{3\times3} & 0_{3\times3} & 0_{3\times3} & \overleftrightarrow{\omega^{(2)}(t)}_{3\times3} & 0_{3\times3} & 0_{3\times3} \\ 0_{3\times3} & 0_{3\times3} & 0_{3\times3} & 0_{3\times3} & 0_{3\times3} & 0_{3\times3} \\ 0_{3\times3} & 0_{3\times3} & 0_{3\times3} & 0_{3\times3} & 0_{3\times3} & \overleftrightarrow{\omega^{(3)}(t)}_{3\times3} \\ 0_{3\times3} & 0_{3\times3} & 0_{3\times3} & 0_{3\times3} & 0_{3\times3} & 0_{3\times3} \end{bmatrix} \tag{57}$$

Continuing, we combine Eqs. (52) and (55) into one equation as follows:

$$\{\delta\dot{X}\} = \{\delta\dot{\tilde{X}}\} + [D]\{\delta\tilde{X}\} \tag{58}$$

The only difficult issue is the nature of the four coordinates used in the analysis. Table 1 presents a summary or the reader may consult Ref. [11].

We formulate the work done in terms of the second column since it contains the proper conjugate to the applied moments. However, the first equation in the bottom rows relates these to the variations of the essential generalized coordinates (whose rates appear in the last column).

We structure the kinetic energy in terms of the third column. However, the second equation at the bottom relates these to the virtual generalized velocities.

Finally, the last equation in the bottom row represents the restriction on the variations of the generalized velocities that must also be included when applying the principle of virtual work.

Principle of Virtual Work. Physicists developed Hamilton's principle for a system with conservative forces. However, engineers developed the principle of virtual work to account for nonconservative forces (viscous damping, applied loads, etc.). To use it, we drop the potential energy and absorb all applied forces (including gravity, despite it being conservative) into the work done on the system.

We list all forces applied to the system

$$\{Q(t)\} = \begin{pmatrix} F_C^{(1)I}(t) \\ M_C^{(1)}(t) \\ F_C^{(2)I}(t) \\ M_C^{(2)}(t) \\ F_C^{(3)I}(t) \\ M_C^{(3)}(t) \end{pmatrix} = \begin{pmatrix} F^{(w)I}(t) + F_b^I - m^{(1)}ge_2 \\ M^{(w)}(t) - M_m^{(t)}(t)e_2 \\ -m^{(2)}ge_2 \\ M_m^{(t)}(t)e_2 - M_m^{(a)}(t)e_1 \\ -m^{(3)}ge_2 \\ M_m^{(a)}(t)e_1 \end{pmatrix} \tag{59}$$

Allow us to interpret the terms

$$\begin{aligned} F^{(w)I} &= \text{force from waves} \\ F_b^I &= \text{force from buoyance} \\ m^{(1)}ge_2 &= \text{force form gravity on the ship} \\ M^{(w)}(t) &= \text{moment from waves} \\ -M_m^{(t)}(t)e_2 &= \text{reverse moment on ship from tower} \\ -m^{(2)}ge_2 &= \text{force from gravity on the tower} \\ M_m^{(t)}(t)e_2 &= \text{moment that turns the tower} \\ -M_m^{(a)}(t)e_1 &= \text{reverse moment on tower from arm} \\ -m^{(3)}ge_2 &= \text{force from gravity on the arm} \\ M_m^{(a)}(t)e_1 &= \text{moment on crane that turns the arm} \end{aligned}$$

The superscript I in $F^{(w)I}$ and F_b^I indicates that the components of the forces are expressed in the inertial frame.

Equation of Motion. By making the substitutions and carrying out the calculus of variations, one obtains the following:

$$[M^*(t)] \equiv [B(t)]^{\mathrm{T}}[M][B(t)] \tag{60a}$$

$$[N^*(t)] \equiv [B(t)]^{\mathrm{T}}\left([M]\left[\dot{B}(t)\right] + [D(t)][M][B(t)]\right) \tag{60b}$$

$$\{F^*(t)\} = [B(t)]^{\mathrm{T}}\{F(t)\} \tag{60c}$$

For arbitrary, virtual essential-displacements, we obtain the system equations of motion

$$|M^*(t)|\{\ddot{q}(t)\} + [N^*(t)]\{\dot{q}(t)\} = \{F^*\} \tag{61}$$

The result is a series of five coupled homogeneous differential equations. In fact, the power of this method is that one need not reformulate the analysis for a more complex multibody cranes system. One needs to only expand the dimensionality of the system. The mathematics remains in block matrix form, ready for computation in software.

Updating the Ship's Rotation Matrix

The rotation matrices for the tower and arm are standard due to their derivation from revolute joint mechanics. However, we must know the rotation matrix of the ship for several reasons. First, it is required in the updating of the B matrix. Second, it is required to apply added mass forces. Finally, we need it for visualization.

We must reconstruct the rotation matrix of the ship from the angular velocity. We must compute the rotation matrix $R^{(1)}(t)$ by solving the following equation:

Table 2 Parameters used in this study

Variable	Applied constant
Mass of ship	$m^{(1)} = 10,000\,\text{kg}$
Mass of tower	$m^{(2)} = 500\,\text{kg}$
Mass of arm	$m^{(3)} = 500\,\text{kg}$
Mass of crane load	$m^{(4)} = 1000\,\text{kg}$
Tower position in the z-axis	$d^{(1)} = -10\,\text{m}$
Tower position in the x-axis	$b^{(1)} = -5\,\text{m}$
Half the height of tower	$l^{(2)} = 3.5\,\text{m}$
Half the length of arm	$l^{(3)} = 3.5\,\text{m}$
Radius of tower	$r^{(2)} = 0.5\,\text{m}$
Radius of arm	$r^{(3)} = 0.5\,\text{m}$
Width of ship	$Lps = 10\,\text{m}$
Length of ship	$Lsb = 20\,\text{m}$
Height of ship	$Lh = 5\,\text{m}$
Torque applied to tower	$M^{(1)} = 100,000\,\text{N}\cdot\text{m}$
Torque applied to arm	$M^{(2)} = 70,000\,\text{N}\cdot\text{m}$
Dampening factor	See results

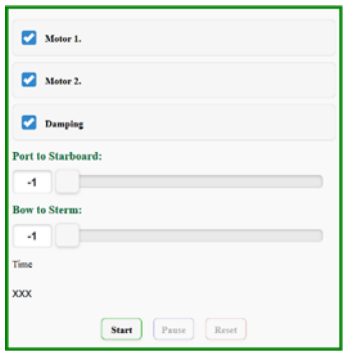

Fig. 4 Control box

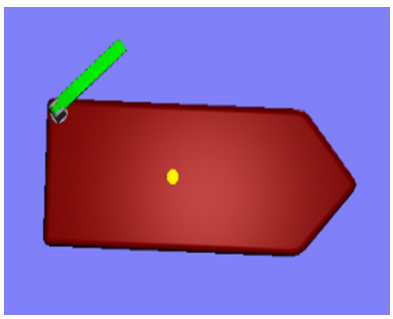

Fig. 5 Motor 1 checked

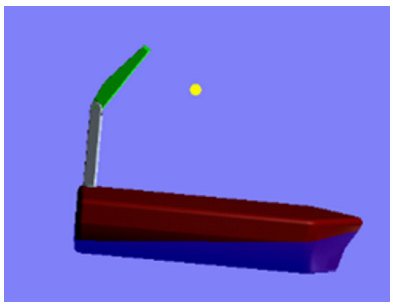

Fig. 6 Motor 2 checked

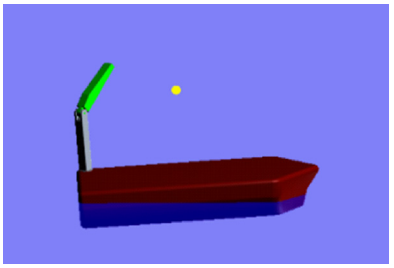

Fig. 7 Motor 1 and motor 2 checked

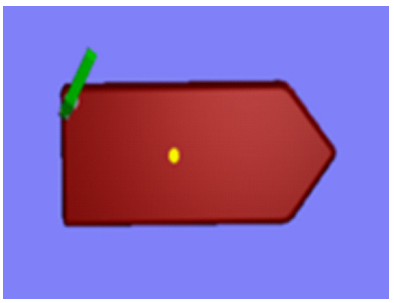

Fig. 8 Motor 1 and motor 2 checked

$$\dot{R}^{(1)}(t) = R^{(1)}\overleftrightarrow{\omega}(1)(t) \tag{62}$$

Let us assume for a moment that $\overleftrightarrow{\omega}(1)(t)$ is constant and is designated as $\overleftrightarrow{\omega}_0$. Then, with initial value $R(0)$, the solution is

$$R^{(1)}(t) = R(0)\exp(t\overleftrightarrow{\omega}_0) \tag{63}$$

There does exist a known analytical, closed-form solution to Eq. (63), but only for cases in which $\overleftrightarrow{\omega}_0$ is constant. It derives from the Cayley Hamilton theorem and is known as the Rodrigues' rotation formula to obtain a series expansion of the exponential of a matrix [18].

Computation

Simplification of the Model. To simplify the calculations, we neglect wave forces and moments. We also ignore gravity and buoyancy in this first pass. We assume the ship is stationary and will only rotate about its mass center due to the motion of the crane arms. Despite this, we have developed the theory to account for all of these in the next phase.

We assume the shape of the ship to be a solid cuboid. We represent the tower and arm as cylinders.

Numerical Integration. In this paper, as a first pass, we use a *very* primitive numerical integration scheme since the goal is edification, visualization, and a first pass. We used a one-step forward Euler integration that, admittedly, becomes unstable relatively early in the computation. We will rectify this in future work by comparing Runge-Kutta and Newmark-Beta. However, the primary goal here is also the full 3D analysis and display on mobile devices with qualitative results.

Damping. In this paper, we used a fictitious viscous damping for all the variables to simulate buoyancy. The moving frame method is new. We desire to show the power of this method which was implemented here by undergraduate students. Since we are keeping it simple, we desire to keep the algorithm simple with regard to hydrostatic effects on the boat. Had we included those effects been precisely included, the numerical integration would

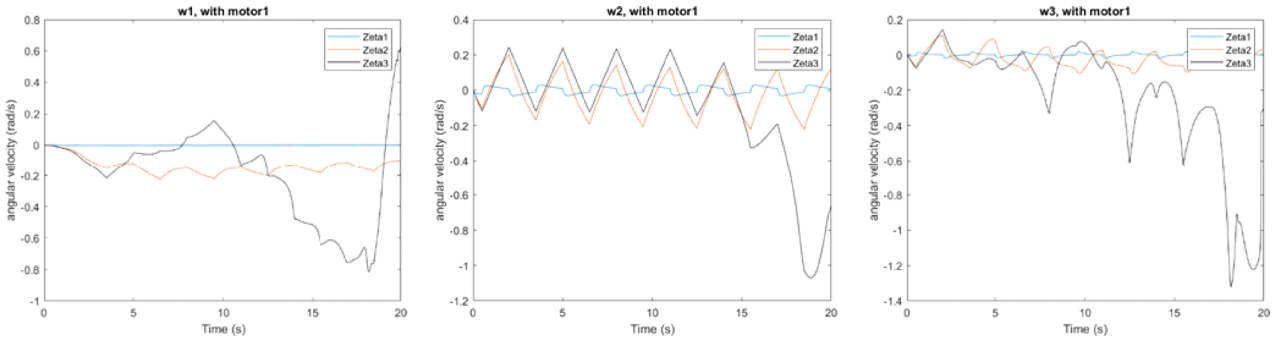

Fig. 9 Pitch, yaw, and roll, with various damping with the tower motor activated

have become unstable, sooner, and voided even these qualitative results. We have shown that the placeholder is present. We will account for these effects in the next phase. In this paper, we will apply a fictitious damping parameter to each of the essential generalized coordinates.

Updating the Rotation Matrix. As stated, the Cayley Hamilton theorem and the resulting Rodriguez equation for updating the rotation matrix are valid only for a constant angular velocity. We can circumvent this by assuming a central difference approximation and a constant angular velocity between time steps. Time limitations in this current work precluded that. Since we were already using a simple numerical integration scheme, there was no loss in assuming a constant angular velocity at the start of each time-step. This will be addressed in the next phase.

Visualization

WebGL is a JavaScript interface for rendering interactive two-dimensional (2D) and 3D computer graphics [19]. WebGL is compatible with the major web browsers such as Chrome, Firefox, Safari, and Opera. It is free and can be used without the need for plugins. It introduces an API which closely conforms to OpenGL ES 2.0, thus being compatible with HTML5.

The webpage was designed with checkboxes for motor1, motor2, damping, and sliders for placement of the crane. This is so the user can control which parameters that are influencing the ship. The ship has full 3D-rotation, hence, a movement made by the crane will affect the behavior of the ship in all axes.

Each motor has been checked to observe qualitative responses. The qualitative responses were in accordance with what would be expected from a physical model, thus the 3D-simulation seems realistic.

It is critical to note that the authors are not pushing a software system. The MFM makes dynamics easy to code. The computations run on cell phones. The reader may proceed to this link on a laptop or mobile device and experiment in the website link.[1]

Parameters Used. Table 2 presents all parameters used in the online simulation.

Results

Qualitative. It has been demonstrated elsewhere [6–8,12,14,18,20–22] that the moving frame method produces the same equations of motion as the traditional approaches to dynamics.

The purpose of this paper is to introduce this MFM to a new community, in the context of a challenging problem. Our only limitation is that we did not encumber and drastically lengthen this presentation with all required details for a physically realistic simulation: wave moments, hydrostatics, wave radiation, and added mass.

Separately, WebGL beckons the arrival of the 3D web. In fact, we are currently working up the MFM to be the first fully interactive, 3D textbook. We envision a future where 3D interactive animations instead of static figures will accompany research papers. This paper calls out to that future by presenting the 3D animations, viewable on cell phones. We feel that, in this case, with a new MFM method, qualitative results are sufficient until the next phase of the work.

Thus, we suggest that the reader to view the animations and interact with them (on laptops or cell phones). To visualize the 3D-motion, click the check-boxes, motor 1, motor 2, and damping (see Fig. 2). As default, the crane is placed in the stern corner. However, the crane can be placed in different positions to see how this affects the ship motion. Then click start. To change the position of the crane, or turn on/off the motors or damping, click reset. Make the changes and click start. Figures 5 and 6 show the animation when only motor 1 is checked. Figures 7 and 8 show the animation when motors 1 and 2 are checked.

Quantitative. This paper regards a new approach to engineering dynamics and presents new research results. We point out, however, that the pedagogical aspects, themselves, present research in a new mathematical approach to dynamics.

There are two approaches to such validation. First, we can focus on numerical validation by comparing the results to an existing software tool. The group will shortly have the funds for this endeavor. Second, we have now commenced the experimental analysis in the HVL wave tank and this is more significant. However, both of those tasks are in themselves ambitious undertakings. A paper that would include that information would border on a textbook. By presenting the theoretical results in a standalone paper, supplemented with some minimal numerical results for the sake of discussion, we feel we can proceed to the next step of combined numerical experimental validation by referring to this work. With that in mind, we present minimal results in Figs. 9–11.

In all figures, the torque of motor 1 rotates the crane tower and the torque of motor 2 rotates the distal crane boom. Table 1 presents the values for the driving torques.

In all figures, damping parameters for the angular velocities of the ship are $\zeta_1 = 500,000\,\text{Nms}$, $\zeta_2 = 25,000\,\text{Nms}$, and $\zeta_1 = 0.0$.

In all figures, the crane was placed at the center of the boat.

In all figures, reading left to right, $w1$ is the pitch, $w2$ is the yaw, and $w2$ is the roll.

We ask the reader to keep in mind that the incipient numerical noise in all figures was due to the relatively large time-step, the poor choice of one-step Euler, and the abrupt and unnatural change in the motor (enabled by the nature of programming, but not entirely realistic).

Figure 9 presents the results when the crane tower rotates. It is to be expected that, in this case, the yaw $w2$ is most significant.

[1] http://home.hib.no/prosjekter/dynamics/2018/crane/

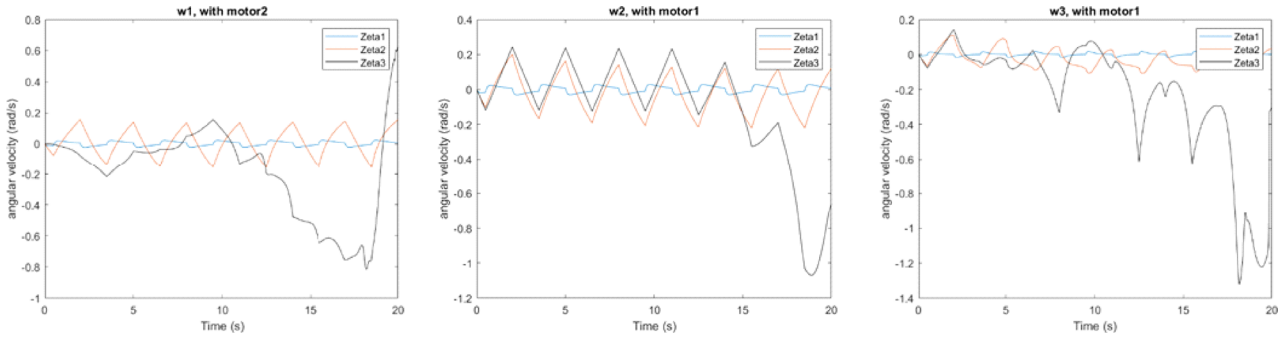

Fig. 10 Pitch, yaw, and roll, with various damping with the distal arm motor activated

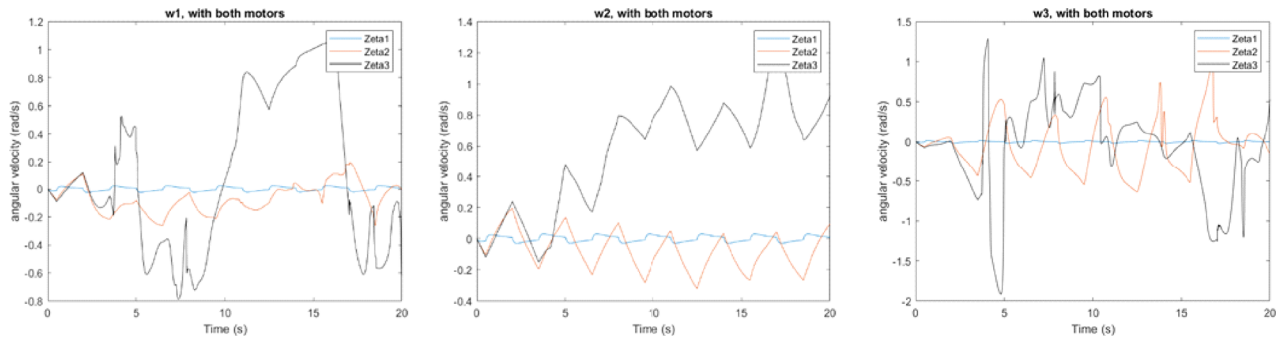

Fig. 11 Pitch, yaw, and roll, with various damping with both motors activated

However, the rotating boom does induce a pitch and roll. In all cases, the damping significantly reduces the magnitudes of the angular velocities.

Figure 10 presents the results when the distal crane arm is lifting. It is to be expected that, in this case, the pitch $w1$ is most significant. In all cases, the damping significantly reduces the magnitudes of the angular velocities.

Figure 11 presents the results when both motors operate. Here, there is limited ability to distinguish the role of each motor. However, it is clear that damping can sufficiently eliminate all motion. The zero-damping case evinces the complex relationships between the two motors.

Finally, we point out that the application of the torques was not entirely realistic. In a real situation, there is a ramp up and a ramp down of the motor. In these cases, there were abrupt changes made possible by the nature of coding. Despite this, during the constant moment phases, the angular velocities are relatively constant. Ongoing work addresses these challenges.

We are already aware that the moving frame method produces the same equations of motion as the traditional method. However, the MFM uses the same notation for 2D, 3D, single bodies, and multibodies; and it obtains the same equations expeditiously, as stated in the references in the Qualitative section [6–8,12, 14,18,20–22].

The MFM method has been validated elsewhere for the analysis of the tennis racket flip [18], flexible robotics [23], and caudal fin analyses [24]. This paper presents the first step in the application of ocean engineering and the analyses of cranes on ships.

Future Work

There are several immediate next steps in this work.

First, future work will involve two alternative and improved numerical integration schemes. We are currently working on using Newmark-Beta methods and a Runge-Kutta method. We will supply both methods with a predictor/corrector algorithm. Then, we will compare both schemes for energy loss. The MFM produces one generalized form of the equations of motion (Eqs. 60(a)–60(c)). This suite holds for other ongoing projects, such as a gyroscopic wave energy converter (20), ROV motion (21), and ship stability (22). Thus, we are leveraging all such projects to discover the most efficient numerical integration scheme.

We will implement the Rodriguez formula by assuming a constant angular velocity, not at the time steps in question, but use a midpoint rule [18].

In addition, we will include wave moments and added mass.

We will prescribe functions to ramp up and ramp down the motor torques, more naturally.

Indeed, these are qualitative results. An additional next step is to assess the model in a wave tank at HVL. This work has commenced.

In the next phase, we will plot the angular momentum sphere and the kinetic energy ellipsoids to show that there exist restrictions (polhodes) on the trace of the angular velocity vector on these surfaces.

In the next pass, we will allow for deformation of the crane arms. This can be done by applying the MFM to the modeling of beams [23].

This brings us to the long-term goals.

Next, one must realize that a qualitative visual analysis is not sufficient. The group has already commenced developing physical models in the HVL wave tank in order to conduct experimental validations.

AI is the study of "intelligent agents"—the study of any device that perceives its environment and takes actions that maximize its chance of success at some goal. At this time, "device" is restricted to mean "computers." However, today's mechanical machines think (with onboard CPUs) and communicate (with IP addresses). Soon, with biologically inspired neural networks, machines will learn. In anticipation of this, simulations of mechanical systems

(dynamics) will enhance adaptive machine learning. The moving frame method is unique in that it is eminently programmable and rapidly deployed in new settings, obviating the need for legacy implementations of multibody dynamics codes extant today.

Thus, the next step in this work is to add learning modules to the evolving software so that ships with onboard sensors can take action depending on conditions or expected conditions from learned behavior.

Conclusions

This work demonstrates the power of the moving frame method for offshore mechanics. This work demonstrates the power of the 3D web to visualize ship mechanics on mobile devices. This paper focused on qualitative results. We emphasize that the achievement here is not simply the analysis in and of itself. Rather, it is also the use of a new method in dynamics and confirmation on 3D web pages. Undergraduate students conducted this work—the math, the coding, and the visualization—and this is testimony to the power of a new method in dynamics.

There are other means to extract the equations of motion for ship mechanics, but none as efficient as the MFM and not as readily programmable.

Nomenclature

$[B]$ = B-matrix
$[D]$ = combined angular velocity matrix
$\{F\}$ = force and moment list
$\{F^*\}$ = generalized force
H = angular momentum
$J_c^{(\alpha)}$ = 3×3 mass moment of inertia matrix
$[M]$ = mass matrix
$[M^*]$ = reduced mass matrix
$[N^*]$ = reduced nonlinear velocity matrix
q = generalized position
$\{\dot{q}\}$ = generalized velocity variable list
$\{\ddot{q}\}$ = generalized acceleration variable list
$\{\dot{X}\}$ = velocity list
$\{\tilde{X}\}$ = virtual displacements
δW = virtual work
$\delta\Pi$ = variation of frame connection matrix
$\overleftrightarrow{\delta\pi}$ = virtual rotational displacement
Ω = time rate of the frame connection matrix
ω = angular velocity vector
$\overleftrightarrow{\omega}$ = skew-symmetric angular velocity matrix

References

[1] MacGregor, 2018, "MacGregor 3-Axis Motion Compensated Cranes," MacGregor Finland Oy, Kaarina, Finland, accessed Sept. 24, 2018, https://www.macgregor.com/Products-solutions/products/offshore-and-subsea-load-handling/3-axis-motion-compensation-cranes/

[2] Rolls-Royce, 2018, "Rolls Royce Marine, Dual Draglink Crane," Rolls-Royce plc, London, accessed Sept. 24, 2018, https://www.rolls-royce.com/products-and-services/marine/product-finder/cranes/subsea-crane/dual-drag-link-crane-subsea.aspx#/

[3] Maczyński, A. A., and Wojciech, S. S., 2011, "Stabilization of Load's Position in Offshore Cranes," ASME. J. Offshore Mech. Artic Eng., **134**(2), p. 021101.

[4] Xu, J., Ren, Z., Li, Y., Skjetne, R., and Halse, K., 2018, "Dynamic Simulation and Control of an Active Roll Reduction System Using Free-Flooding Tanks With Vacuum Pumps," ASME J. Offshore Mech. Arct. Eng., **140**(6), p. 061302.

[5] Kongsberg Gruppen ASA, 2018, "Autonomous Ship Project, Key Facts About YARA Birkeland," Kongsberg Gruppen ASA, Kongsberg, Norway, accessed Sept. 24, 2018, https://www.km.kongsberg.com/ks/web/nokbg0240.nsf/AllWeb/4B8113B707A50A4FC125811D00407045?

[6] Nordvik, A., Khan, N., Burcă, R. A., and Impelluso, T. J., 2017, "A Study of Roll Induced by Crane Motion on Ships: A Case Study of the Use of the Moving Frame Method," ASME Paper No. IMECE2017-70111.

[7] Impelluso, T., 2016, "Rigid Body Dynamics: A New Philosophy, Math and Pedagogy," ASME Paper No. IMECE2016-65970.

[8] Impelluso, T., 2017, "The Moving Frame Method in Dynamics: Reforming a Curriculum and Assessment," Int. J. Mech. Eng. Educ., **46**(2), pp. 158–191.

[9] Cartan, É., 1986, *On Manifolds With an Affine Connection and the Theory of General Relativity*, Bibiliopolis, Napoli, Italy.

[10] Frankel, T., 2012, *The Geometry of Physics, an Introduction*, 3rd ed., Cambridge University Press, New York.

[11] Murray, R. M., Li, Z., and Sastry, S. S., 1994, *A Mathematical Introduction to Robotic Manipulation*, CRC Press, Boca Raton, FL.

[12] Murakami, H., 2013, "A Moving Frame Method for Multibody Dynamics," ASME Paper No. IMECE2013-62833.

[13] Denavit, J., and Hartenberg, R., 1955, "A Kinematic Notation for Lower-Pair Mechanisms Based on Matrices," ASME J. Appl. Mech., **22**, pp. 215–221.

[14] Murakami, H., 2015, "A Moving Frame Method for Multi-Body Dynamics Using SE(3)," ASME Paper No. IMECE2015-51192.

[15] Wittenburg, J., 1977, *Dynamics of Rigid Bodies*, B. G. Teubner, ed., ZAMM, Weinheim, Germany.

[16] Wittenburg, J., 2008, *Dynamics of Multibody Systems*, 2nd ed., Springer, Berlin.

[17] Holm, D. D., 2008, *Geometric Mechanics, Part II: Rotating, Translating and Rolling*, World Scientific, Hackensack, NJ.

[18] Rios, O., Murakami, H., and Impelluso, T., 2017, "A Theoretical and Numerical Study of the Dzhanibekov and Tennis Racket Phenomena," ASME J. Appl. Mech., **83**(11), p. 111006.

[19] Khronos Group, 2018, "OpenGL ES for the Web," The Khronos Group Inc., Beaverton, OR, accessed Sept. 24, 2018, https://www.khronos.org/webgl/

[20] Norbach, A., Fjetland, K., Hestetun, G., and Impelluso, T., 2018, "Gyroscopic Wave Energy Converter for Fish Farms," ASME Paper No. IMECE2018-86188.

[21] Austefjord, K., Hestvik, M., and Laresen, L., 2018, "Modeling Subsea ROV Motion Using the Moving Frame Method," Int. J. Dyn. Control (in press).

[22] Flatlandsmo, J., Torbjørn, S., Halvorsen, Ø., and Impelluso, T., 2018, "Modeling Stabilization of Crane and Ship by Gyroscopic Control Using the Moving Frame Method," ASME J. Comput. Non-Linear Dyn., **14**(3), p. 031006.

[23] Rios, O., 2016, "Development of Active Mechanical Models for Flexible Robots to Duplicate the Motion of Inch Works and Snakes," ASME Paper No. IMECE2016-65550.

[24] Murakami, H., 2016, "Modeling and Experimentation of a Ribbed Caudal Fin for Aquatic Robots," ASME Paper No. IMECE2017-71235.